PCCP

Accepted Manuscript

ROYAL SOCIETY OF CHEMISTRY

www.rsc.org/pccp

Phys. Chem. Chem. Phys.

RSCPublishing

ARTICLE

Effect of ozone exposure on the electrical characteristics of high-purity, large-diameter semiconducting carbon nanotubes

Cite this: DOI: 10.1039/xoxxoooooox

Received ooth ,
Accepted ooth

DOI: 10.1039/xoxxoooooox

www.rsc.org/

Jia Gao and Yueh-Lin (Lynn) Loo*

In this study, we have elucidated the interactions between ozone and carbon nanotubes by monitoring the characteristics of field-effect transistors based on polymer-sorted, large-diameter semiconducting carbon nanotubes. The drain-source current of these transistors initially increases with ozone exposure; it then progressively decreases with increasing exposure beyond 3 min. This non-monotonic dependence of the drain-source current can be ascribed to two competing processes. At short ozone exposures, p-doping of carbon nanotubes dominates; the drain-source current thus increases as a result of increasing hole concentration. This effect is most evidenced in a progressive threshold voltage shift towards positive voltages with increasing exposure to ozone. At extended ozone exposures, chemical oxidation of carbon nanotubes instead dominates. The drain-source current decreases as a result of decreasing hole mobility. This effect manifests itself in a monotonic decrease in mobility of these devices as a function of ozone exposure.

Introduction

Single-walled carbon nanotubes (SWCNTs) have attracted tremendous research interest in physics and material science in the last two decades. The processing and modification of carbon nanotubes provide tunability of its properties and have been exploited in many applications.[1-3] Ultraviolet (UV) ozone treatment is one of the most appealing techniques for chemical functionalization of carbon nanotubes because of its simplicity, low-temperature operation and controllability, etc.[4-6] Ozone has also been widely used for the purification, processing and patterning of carbon nanotubes for electronic applications.[7-8] A number of studies of ozone exposure on the electrical conductivity of SWCNT network have been carried out in the last few years. On the one hand, several reports demonstrate that ozone exposure disrupts conjugated pi-bonds and removes electronic states near the Fermi level of carbon nanotubes; this process results in a decrease in the nanotube network conductivity.[9-11] On the other hand, an increase in conductivity upon ozone exposure has also been reported; this observation has been attributed to charge transfer from the carbon nanotubes to adsorbed ozone.[12] Consistent with this picture, first-principles calculations show an appreciable binding energy between ozone and carbon nanotubes.[13] This interaction results in a peak state near the Fermi level, effectively making ozone a p-dopant for carbon nanotubes.[14] More recently, Ma and coworkers demonstrated that the resistance of carbon nanotube arrays can be tuned by changing the concentration of ozone during exposure. Specifically, the resistance decreases upon exposure to ozone generated in air whereas it increases dramatically when exposed to higher concentrations of ozone.[15] Taking these examples collectively, the electronic properties of carbon nanotubes must be affected by exposure to ozone in non-trivial ways. Given the non-monotonicity of carbon nanotube resistance with ozone exposure observed by Ma and coworkers, we postulate that both effects, i.e., doping and chemical oxidation, must take place concurrently and competitively. A precise evaluation of the relative dominance of either effect, however, has not yet been reported. Importantly, the carbon nanotube networks used in these studies have comprised both metallic and semiconducting

tubes. Such electronic heterogeneity has further complicated our understanding of the interactions between ozone and carbon nanotubes.

In this study, we focus on understanding the interactions between ozone and semiconducting carbon nanotubes by evaluating the electrical characteristics of polymer-sorted, large-diameter semiconducting SWCNT-based transistors. We observe positive shifts in the threshold voltage and a concurrent decrease in hole mobility with increasing ozone exposure, allowing us to evaluate the relative dominance of these two competing effects of ozone exposure on the electrical properties of carbon nanotubes.

Results and discussion

Figure 1 contains the optical absorption spectra of polymer- and surfactant-sorted SWCNT dispersions normalized at their second optical transition of semiconducting carbon nanotubes at 1013 nm (E_{S22}).

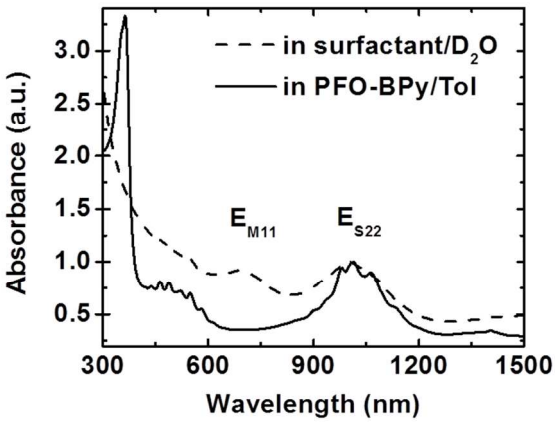

Fig. 1 Optical absorption spectra of surfactant dispersed (dashed line) and polymer-sorted carbon nanotubes (solid line) normalized at the E_{S22} transition. The absorbance in the 620-820 nm range, designated E_{M11}, corresponds to the optical transitions of metallic tubes.

The absorption spectrum of the polymer-sorted SWCNT dispersion (solid line) shows lower background intensity and better-resolved features compared to that of the surfactant-sorted SWCNT dispersion (dashed line). This observation indicates that sorting SWCNTs with PFO-BPy, as opposed to sodium cholate, more effectively isolates individual tubes in solution.[16] Importantly, the spectrum of the polymer-sorted SWCNT dispersion also shows substantially lower absorbance in the 620-820 nm range. Absorption in this region corresponds to the optical transition of metallic tubes (E_{M11}). This observation thus evidences that sorting with PFO-BPy preferentially selects for semiconducting SWCNTs compared to sorting with sodium cholate, which shows no selectivity.

Figure 2(a) shows the Raman spectrum of polymer-sorted SWCNT network in the channel regions of the transistors before ozone exposure; the peak intensities of the D and G bands as a function of ozone exposure time are compiled in Figure 2(b).

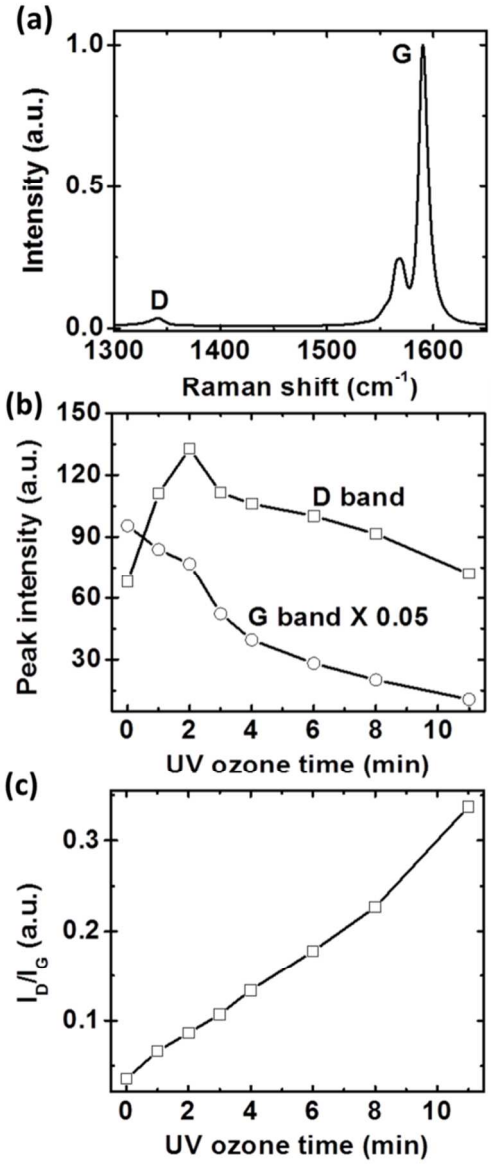

Fig. 2 Raman spectrum of carbon nanotube network before ozone exposure (a); variation of D and G peak intensities (b) and I_D/I_G ratio (c) extracted from the Raman spectra of SWCNT network with ozone exposure.

The G band at 1590 cm^{-1} is attributed to tangential mode vibrations of the carbon atoms in the SWCNTs while the D band at 1340 cm^{-1} is attributed to the presence of defects and other disorder in the SWCNTs.[17] For comparison, we have also plotted the intensity ratio, I_D/I_G, as a function of ozone treatment time in Figure 2(c). We observe an initial increase in the D-band intensity at short ozone exposure, and then a steady decrease in its intensity beyond 2 minutes of exposure. The intensity of the G band attenuates monotonically upon ozone exposure. The ratio of D and G band intensities, I_D/I_G, which is

often used as a proxy for the defect density of carbon nanotubes,[18-20] increases monotonically upon ozone exposure. These observations indicate a progressive increase in defect density of the carbon nanotubes with ozone exposure, attributable to chemical oxidation of SWCNTs.[9]

Prior work examining the effects of ozone exposure on carbon nanotubes have used unsorted carbon nanotube networks. Given that electrical conductivity was the primary parameter tracked in these measurements and the electrical conductivity of metallic carbon nanotubes is orders of magnitude higher than those of semiconducting nanotubes, the researchers were primarily measuring the effects of ozone exposure on metallic carbon nanotubes. That we have access to pre-sorted carbon nanotubes has allowed us to evaluate the impact of ozone exposure on the electrical characteristics of semiconducting carbon nanotubes. To do so, we have constructed FETs and measured the electrical characteristics of these devices as a function of ozone exposure. Figure 3 summarizes the electrical characteristics of a polymer-sorted SWCNTs network-based transistor with a 20-μm channel length.

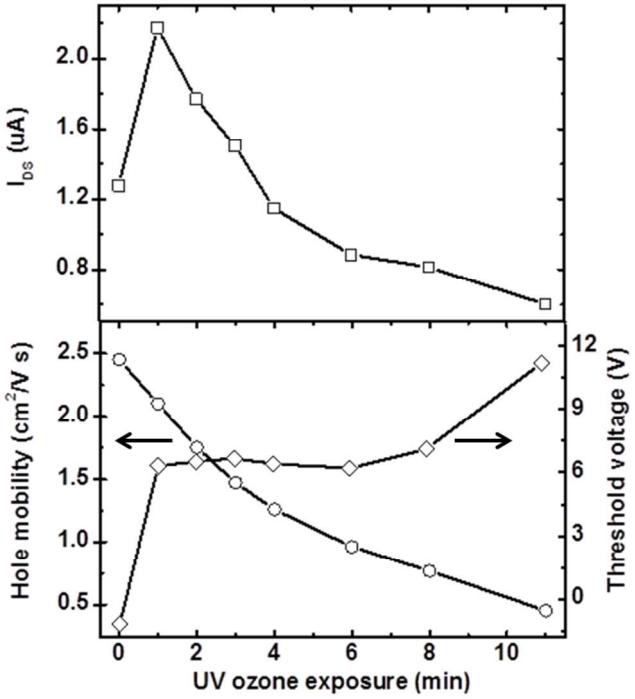

Fig. 3 Source-drain current of a SWCNT-network FET having 20 μm channel length at V_G = -10 V (a); hole mobility and threshold voltage as a function of ozone exposure (b).

The source-drain current (I_{DS}) of the transistor at a gate bias -10V is shown in Fig. 3(a). We observe a non-monotonic dependence of I_{DS} on ozone exposure time. Specifically, I_{DS} increases from 1.28 μA to 2.17 μA after 1 min of ozone exposure; it then decreases to 1.5 μA after 3 min. Extended exposure results in a further decrease of current to 0.6 μA at 11 min. Like the electrical conductivity of unsorted carbon nanotube networks studied by Ma and coworkers,[15] I_{DS} appears to depend non-monotonically on ozone exposure. We believe this non-monotonic dependence to arise from the same two competitive processes that governed the conductivity dependence on ozone concentration observed by Ma and coworkers. To evaluate, we extracted the hole mobility and threshold voltage (V_{th}) of the transistor and tracked these parameters as a function of ozone exposure as shown in Fig. 3(b). The hole mobility, u, was extracted per equation (1) below:

$$u = g_m \times \frac{L}{W} \times \frac{1}{C_{ox}} \times \frac{1}{V_{DS}} \qquad (1)$$

where g_m is the transconductance, V_{DS} is the drain-source voltage, and L and W are the channel length and width of the transistor, respectively. We used 300-nm thick thermally grown silicon dioxide as our gate dielectric; the capacitance, C_{ox}, of which is 11.5 nF/cm^2. V_{th} was extracted using extrapolation-in-the-linear-region (ELR) method. [21]

Before ozone exposure, the FET exhibits an extracted hole mobility of 2.45 cm^2/Vs. This value is on par with those reported in the literature for other polymer-sorted carbon nanotubes network-based transistors.[22-24] To account for the coverage of SWCNTs within the channel region, we also estimated the hole mobility of the transistor using an effective capacitance[25] extracted per equation 2 below:

$$C_{eff} = \{C_Q^{-1} + \frac{1}{2\pi\varepsilon_0\varepsilon_{ox}} \ln[\frac{\Lambda_0}{R}\frac{\sinh(2\pi t_{ox}/\Lambda_0)}{\pi}]\}^{-1}\Lambda_0^{-1} \qquad (2)$$

where Λ_0^{-1}represents the linear density of SWNTs, C_Q is the quantum capacitance of nanotube, $C_Q \approx e^2 g \approx 2.3$, in which g is the electron density of states of the nanotubes, [26] ε_{ox} is the dielectric constant of SiO_2, t_{ox} is the oxide thickness and R is the diameter of the nanotube (1.4 nm). Based on equation (2), the effective capacitance was estimated to be 10.4 nF/cm^2, or approximately 10% lower than the capacitance of the thermally grown silicon dioxide alone. Accordingly, the hole mobility estimated using the effective capacitance should be approximately 10% higher, but still within the ball park of what had been reported for similar devices. Independent of the model used to extract hole mobility, we observe a monotonic decrease in this quantity with ozone exposure. Specifically, the hole mobility decreases from 2.45 cm^2/Vs to 0.45 cm^2/Vs after 11 min. of ozone exposure. This decrease can be attributed to chemical oxidation of the carbon nanotubes, which in turn creates defects that disrupts the conducting pathway within the channel region of the transistor. Consistent with a previous study, we thus ascribe the decrease in hole mobility to a decrease in the density of states of the carbon nanotubes near the Fermi level with oxidation.[9]

The threshold voltage, on the other hand, increases from -1.2 V to 6.3 V after 1 min of ozone exposure, and to 6.7 V after 8

min. of ozone exposure. V_{th} further shifts to 11.2 V at 11 min. of ozone exposure. This increase in V_{th} is ascribed to an increase in carrier concentration, likely due to p-doping of the carbon nanotubes during ozone exposure.[27] After an 11-min. ozone treatment, the total shift in threshold voltage is 12.4 V. Given the effective capacitance of 10.4 nF/cm^2, this shift corresponds to an increase in the hole concentration by 8.1 X 10^{11}/cm^2 in the carbon nanotube network in the FET channel with 11 min. of ozone exposure.

That the hole mobility decreases while the threshold voltage simultaneously increases sheds light on the non-monotonic dependence of the drain-source current as a function of ozone exposure. Given that I_{DS} is a product of u and V_{th}, the non-monotonic dependence of I_{DS} with ozone exposure suggests that p-doping dominates the electrical characteristics of semiconducting SWCNTs at short ozone exposures while chemical oxidation of the carbon nanotubes dominates beyond 3-min. of ozone exposure. I_{DS} plummets as a consequence of a drastic decrease in hole mobility beyond 3 min. of ozone exposure. Our control experiments with polymer-only devices reveal PFO-BPY to be electrically insulating; its presence does not contribute to carrier transport in devices based on SWCNT networks.

We can further examine the extent with which chemical oxidation takes place with these semiconducting SWCNT networks. To this end, we have plotted in Figure 4 g_m of polymer-sorted SWCNTs network-based FETs with different channel lengths as a function of I_D/I_G.

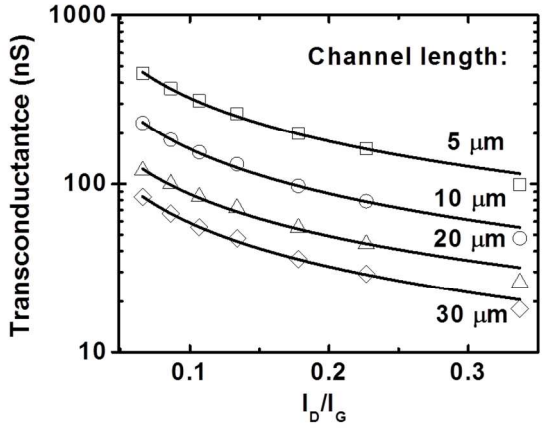

Fig. 4 Transconductance of SWCNT FETs with different channel lengths as a function of I_D/I_G. The solid lines are power law fits to the data.

These devices are well behaved under bias; of 30 devices with varying channel lengths we examined, the average hole mobility was 2.31±0.35 cm^2/Vs before exposure to ozone. Exposure to ozone leads to a uniform decrease in g_m with increasing I_D/I_G. Given that chemical oxidation destroys pi-conjugation along the carbon nanotubes, and such structural defects degrade charge transport, this decrease in g_m with increasing I_D/I_G is not surprising. In fact, this decrease can be described by an empirical power law that has allowed us to correlate the electrical characteristics of these devices with the photophysical properties of the SWCNTs in the device channel:

$$g_m = a \times \left(\frac{I_D}{I_G}\right)^b \quad (3)$$

where a is the prefactor and b is the exponent. The solid lines in Figure 4 represent fits of equation (3) to the data. Fitting the data yields a power coefficient b of -0.85 ± 0.03 that is independent of channel length. Given that the channel lengths of our devices, ranging from 5 to 30 μm, are much larger than the average length of our polymer-sorted SWCNTs (560 nm), the number density of nanotube-nanotube junctions within the active channel should scale with the channel length. Yet, the fact that the same power law having an invariant exponent can be used to fit the electrical characteristics of our devices having different channel lengths suggests that chemical oxidation during ozone exposure occurs uniformly along the carbon nanotubes, as opposed to preferentially affect the tube junctions alone. The morphology of polymer-coated SWCNT network upon ozone exposure was also characterized by scanning electron microscope (SEM) and atomic force microscopy (AFM), and no noticeable change was observed with ozone treatment. A previous study (3) suggests that low-dose O3 reaction with SWCNTs is limited to surface chemical reactions, producing epoxide adducts or ethers, none of which can be easily detected through structural and morphological characterization of the carbon nanotubes. X-ray photoelectron spectroscopy (XPS) was used to assess the surface chemical changes that take place on ozone exposure. We observed an increase in the ratio of oxygen (O1s) to carbon (C1s) intensities with ozone exposure time, along with the emergence of a higher energy shoulder in the C1s region at 288 eV; both observations suggest the formation of C-O and C=O adducts, consistent with what was proposed. (3).

Conclusions

In conclusion, we have decoupled the contributions of two competing processes that take place when semiconducting carbon nanotubes are exposed to ozone by evaluating their field-effect electrical properties. Ozone-doping, which increases carrier concentration, dominates early electrical characteristics, while chemical oxidation, which degrades charge transport, dominates the electrical characteristics of carbon nanotube FETs during later stages of ozone exposure. An empirical law allows straightforward correlation of the electrical characteristics of SWCNT FETs with the photophysical properties of the carbon nanotubes. That the same empirical correlation can be applied to the electrical characteristics of FETs with varying channel lengths suggests that oxidation occurs uniformly along the carbon nanotubes. Our results provide processing-structure-function relationships that govern ozone treatment of carbon nanotubes and suggest tuning of

carbon nanotube electrical properties can be achieved through controlled ozone exposure.

Experimental section

Preparation of dispersion

Polymer-sorted SWCNT dispersions were prepared following the procedure demonstrated by Mistry et al.[28] Arc-discharge carbon nanotubes and poly[(9,9-dioctylfluorenyl-2,7-diyl)-alt-co-(6,6'-{2,2'-bipyridine})]), PFO-BPy, were obtained from Nanolab and American Dye Source, respectively. The solution, comprising 10 mL toluene with 45 mg of SWCNTs and 45 mg of polymer, was sonicated for 30 min. We adopted a two-step ultracentrifuge process per Bisri et al. to extract the polymer-wrapped semiconducting-enriched carbon nanotubes, and then to further remove excess polymer from the sorted tubes.[24]
For comparison, we also made surfactant-dispersed SWCNTs by adding 2 mg of raw carbon nanotubes in 20 mL sodium cholate solution in D_2O (1 wt%), then sonicated for 30 min. and followed by ultracentrifugation at 20,8000 G for 1 h. While the introduction of surfactant can disperse the SWCNTs, this process does not preferentially sort for SWCNTs with select electrical properties.

Device fabrication

Bottom-gate field-effect transistors (FETs) comprising polymer-sorted SWCNT networks were fabricated on heavily doped Si substrate with a thermally grown 300-nm thick silicon dioxide as gate dielectric. Contact pads Ti (5 nm)/Au (50 nm) were defined by standard photolithography, electron-beam evaporation and lift-off. To achieve a uniform CNT network on the Si/SiO_2 substrate, the SiO_2 surface was modified by immersing the substrate in a 0.1 wt% poly-L-lysine solution for 5 min. followed by rinsing with water.[29] The substrate was then soaked in the SWCNT dispersion overnight. E-beam lithography was performed to define palladium (70 nm) source/drain electrodes and to make electrical connections to the contact pads. A final photolithography step was performed to pattern the active channel region. Oxygen plasma treatment removed the SWCNTs outside the channel region and isolated neighboring devices electrically. The SWCNT network in the channel region was protected during this plasma treatment step with photoresist.

Instruments

Ozone was generated in air using an UVO-Cleaner® 42 manufactured by Jelight, Inc. having a lamp intensity of 28 mW/cm^2. At this condition, the steady-state ozone concentration is approximately 500 ppm. Absorbance measurements were performed on a Varian Cary 5000 spectrometer. Raman spectroscopy was performed using a Horiba ARAMIS Raman spectrometer with an excitation wavelength of 532 nm.

Electrical characterization

I-V characterization of polymer-sorted SWCNT network transistors was performed in vacuum (< 5 X 10^{-5} torr) after each ozone exposure and Raman measurement using an Agilent 4155C semiconductor parameter analyzer. The device channel width is 80 μm and the channel length varies from 5 to 30 μm.

Acknowledgements

JG acknowledges the Netherlands Organisation for Scientific Research (NWO) for a Rubicon Post-doctoral Fellowship (Research Grant 680-50-1202). We acknowledge funding from NSF's Division of Chemistry (CHE-1124754) and from NRI (Gift # 2011-NE-2205GB) under the Nanoelectronics Beyond 2020 Initiative. We thank Prof. Schwartz and Conor Thomas for their help with XPS measurements and analysis of the results. We also thank Prof. R. K. Prud'homme and Prof. T. E. Shenk at Princeton University for access to their centrifuge facilities.

.

Notes and references

Department of Chemical and Biological Engineering, Princeton University, Princeton, New Jersey 08544, United States. E-mail address: lloo@princeton.edu; Phone: +1 609 258 9091; Fax: +1 609 258 0211

1. S. Banerjee, T. Hemraj-Benny and S. S. Wong, *Adv. Mater.* 2005, **17**, 17-29.
2. A. Hirsch and O. Vostrowsky, *Top. Curr. Chem.* 2005, **245**, 193-237.
3. J. Cheng, K. A. Fernando, LM. Veca, YP. Sun, AI. Lamond, YW. Lam and SH. Cheng, *ACS Nano* 2008, **2**, 2085-2094.
4. L. Cai, J. L. Bahr, Y. Yao and J. M. Tour, *Chem. Mater*. 2002, **14**, 4235-4241.
5. Y. S. Min, E. J. Bae and W. Park, *J. Am. Chem. Soc.* 2005, **127**, 8300–8301.
6. S. Ghosh, S. M. Bachilo, R. A. Simonette, K. M. Beckingham and R. B. Weisman, *Science* 2010, **330**, 1656-1659.
7. S.-C. Kung, K. C. Hwang and N. Lin, *Appl. Phys. Lett*. 2002, **80**, 4819-4821.
8. Y. Su, S. Pei, J. Du, W. B. Liu, C. Liu and H. M. Cheng, *Carbon* 2013, **53**, 4-10.
9. J. M. Simmons, B. M. Nichols, S. E. Baker, M. S. Marcus, O. M. Castellini, C. –S. Lee, R. J. Hamers and M. A. Eriksson, *J. Phys. Chem. B* 2006, **110**, 7113-7118.
10. L. C. Teaguea, S. Banerjeeb, S. S. Wong, C. A. Richter, B. Varughese and J. D. Batteas, *Chem. Phys. Lett*. 2007, **442**, 354-359.
11. S. Kim, H. –J. Kim, H. R. Lee, J. –H. Song, S. N. Yi and D. H. Ha, *J. Phys. D* 2010, **43**, 305402.
12. W. Wongwiriyapan, S. Honda, H. Konishi, T. Mizuta, T. Ikuno, T. Ohmori, T. Ito, R. Shimazaki, T. Maekawa, K. Suzuki, H. Ishikawa, K. Oura and M. Katayama, *Jpn. J. Appl. Phys*. 2006, **45**, 3669-3671.

13. S. Picozzi, S. Santucci, L. Lozzi, C. Cantalini, C. Baratto, G. Sberveglieri, I. Armentano, J. M. Kenny, L. Valentini and B. Delley, *J. Vac. Sci. Technol. A* 2004, **22**, 1466-1470.
14. S. H. Jhi, S. G. Louie and M. L. Cohen, *Phys. Rev. Lett.* 2000, **85**, 1710-1713.
15. R. Ma, D. Yoon, K. –Y. Chun and S. Baik, *Chem. Phys. Lett*. 2009, **474**, 158-161.
16. A. V. Naumov, S. Ghosh, D. A. Tsyboulski, S. M. Bachilo and R. B. Weisman, *ACS Nano* 2011, **5**, 1639–1648.
17. M. S. Dresselhaus, G. Dresselhaus, R. Saito and A. Jorio, *Phys. Rep*. 2005, **409**, 47-99.
18. M. E. Itkis, D. E. Perea, R. Jung, S. Niyogi and R. C. Haddon, *J. Am. Chem. Soc*. 2005, **127**, 3439-3448.
19. M. A. Pimenta, A. Jorio, S. D. M. Brown, A. G. Souza, G. Dresselhaus, J. H. Hafner, C. M. Lieber, R. Saito and M. S. Dresselhaus, *Phys. Rev. B* 2001, **64**, 041401.
20. H. Murphy, P. Papakonstantinou and T. I. T. Okpalugo, *J. Vac. Sci. Technol. B* 2006, **24**, 715-720.
21. A. Ortiz-Condea, F. J. Garcıa Sancheza, J. J. Liou, A. Cerdeirac, M. Estrada and Y. Yue, *Microelectron. Reliab*. 2002, **42**, 583-596.
22. M. Ganzhorn, A. Vijayaraghavan, A. A. Green, S. Dehm, A. Voigt, M. Rapp, M. C. Hersam and R. A. A. Krupke, *Adv. Mater.* 2011, **23**, 1734-1738.
23. N. Izard, S. Kazaoui, K. Hata, T. Okazaki, T. Saito, S. Iijima and N. Minami, *Appl. Phys. Lett*. 2008, **92**, 243112.
24. S. Z. Bisri, J. Gao, V. Derenskyi, W. Gomulya, I. Iezhokin, P. Gordiichuk, A. Herrmann and M. A. Loi, *Adv. Mater*. 2012, **24**, 6147–6152.
25. Q. Cao, M. Xia, C. Kocabas, M. Shim, J. A. Rogers and S. V. Rotkin, *Appl. Phys. Lett*. 2007, **90**, 023516.
26. S. Rosenblatt, Y. Yaish, J. Park, J. Gore, V. P. L. Sazonova and P. L. McEuen, *Nano Lett*. 2002, **2**, 869–872.
27. S. M. Sze, *Physics of Semiconductor Devices*, Wiley-Interscience, New York, 1981.
28. K. S. Mistry, B. A. Larsen and J. L. Blackburn, *ACS Nano* 2013, **7**, 2231–2239.
29. T. Takahashi, K. Takei, A. G. Gillies, R. S. Fearing and A. Javey, *Nano Lett*. 2011, **11**, 5408−5413.

